

Numerical Investigation of Hydromagnetic Hybrid Cu – Al₂O₃/Water Nanofluid Flow over a Permeable Stretching Sheet with Suction

R.Sindhu

Abstract:

A novel idea of hybrid nanofluid along with an enhanced mathematical model for thermal properties of the hybrid nanofluid is introduced in the current analysis. Hybrid nanofluid belongs to the category of improved heat transfer fluids that have been utilized for augmentation of the heat transfer process. Two types of fluid, namely, hybrid nanofluid Cu – Al₂O₃/water and Nano fluid Cu/water are considered to discuss the physical behavior of the flow and heat transfer in a magnetic field over a stretching sheet in the presence of magnetic field. The impact of varying values of physical parameters and other significant physical quantities has been discussed. It has been seen that the heat transfer rate of hybrid nanofluid Cu – Al₂O₃/water is greater than the heat transfer rate of Nanofluid Cu/water with respect to magnetic field. More combinations of different nano-composites can be tried as to the desired heat transfer rate can be obtained.

Keywords:

Nanofluid, MHD, Suction, hybrid nanofluid, nanoparticles.

Introduction:

In previous decades, a variety of innovative methods have been employed to increase the rate of heat transfer and achieve higher levels of thermal efficiency. Enhancing thermal conductivity is crucial to this process. As a result, numerous efforts have been made to incorporate solid particles with high thermal conductivity into liquids to boost thermal conductivity, leading to the development of nanofluids since the early 1990s. A significant amount of research has been conducted on nanofluids to meet the demands of industrial applications. Although nanofluids satisfy engineers' and scientists' desire for thermal efficiency, better sort of fluid is still being sought for today. Advanced nanofluids with higher thermal conductivity than nanofluids, such as "hybrid nanofluids," have emerged as a solution to these problems. As a result, the authors' main goal in this work is to increase the rate of heat transmission by using hybrid nanofluids.

The affordability, long-term stability, and good fluidity are the three most important prerequisites for the use of nanofluids in real-world heat transfer applications. Oxide nanoparticles, which have achieved mass production, are now widely used by researchers as alternatives to carbon nanomaterials and metal nanoparticles. Regrettably, oxide nanoparticles have a lower heat conductivity than metal nanoparticles.

and it is necessary to overcome the high-volume fraction suspension of oxide particles $\delta > 5.0$ vol.%. attain the necessary increase in heat conductivity. The only method to keep the fluidity good is to reduce the particle concentration. In other words, oxide particles cannot meet the current criteria and finding new nanoparticle with low cost and high performance is still the most important challenge in the area of nanofluids. In order to make it economical, a new type of hybrid nanofluid is used. The incorporation of small amount of metal nanoparticles/nanotubes into an oxide/metal nanoparticles which is already suspended in a base fluid can significantly improve the thermal properties. The benefits of "hybrid nanofluid" are high effective thermal conductivity, improved heat transfer, stability, advantages and disadvantages of individual suspension, attributed to good aspect ratio and synergistic effect of nanomaterials. The

high thermal conductivity of nano- fluids translates into higher energy efficiency, better performance and lower operating costs.

Application areas of hybrid nanofluids are varied widely in almost all the fields of heat transfer such as electronic cooling, engine cooling/vehicle thermal management, generator cooling, coolant in machining, welding, nuclear system cooling, lubrication, thermal storage, solar heating, cooling and heating in buildings, transformer cooling, biomedical, drug reduction, heat pipe, refrigeration, defense, space aircrafts and ships. As far as hybrid nanofluid applications in the industry are concerned, they have better efficiency than that of nanofluids.

These characteristics attracted many researchers to work toward hybrid nanofluids. Many experimental studies have made remarkable results from the usage of these types of hybrid nanofluid systems. Nihara [1] established a nanocomposite that enhances thermal properties through a new material structure concept. Jana et al. [2] noticed the improvement of fluid thermal conductivity by the single and hybrid nano additives. Suresh et al. [3] conducted a study on hybrid nanofluids. The nano mixture they developed was based on a newly created nanomaterial concept and significantly improved thermal properties. An experimental investigation of laminar mixed convection in an inclined tube using an (Al₂O₃–water) hybrid nanofluid was carried out by Momin [4]. Following this, Suresh et al. [5] examined the heat transfer performance of (Al₂O₃–Cu/water) hybrid nanofluid. Baghbanzadeh et al. [6] examined the synthesis of spherical silica/multi-walled carbon nanotube hybrid nanostructures and evaluated the thermal conductivity of the corresponding nanofluids.

Over the past few decades, issues related to hydromagnetic nanofluids have gained increasing industrial importance. Engineering applications such as gas turbines and propulsion systems used in aircraft, missiles, satellites, and space vehicles highlight their relevance. At elevated operating temperatures, magnetohydrodynamic (MHD) heat transfer effects become highly significant. Additionally, the study of flow over stretching sheets is commonly encountered in practical situations. These problems have gained significant attention from researchers because of their wide-ranging importance in areas such as microelectronics, microfluidics, transportation, manufacturing, medicine, space technology, acoustics, and avionics. Sparrow et al. [7] were among the first to examine the influence of a magnetic field on natural convection heat transfer. Crane [8] later analyzed fluid flow over a stretching plate. Subsequently, Andersson and Dandapat [9] explored the behavior of power-law fluid flow across a stretching sheet. Chakrabarti and Gupta [10] investigated hydromagnetic flow and associated heat transfer over a stretching surface. Further, Vajravelu [11] provided a detailed analysis of hydromagnetic convective flow over a continuously moving surface. Das et al. [12] also contributed to this area of research.

2. Formulation of the problem:

A two-dimensional, steady, nonlinear, laminar boundary-layer flow of an electrically conducting, incompressible, viscous hybrid nanofluid over a stretching sheet is examined. The analysis incorporates suction and the influence of a magnetic field. The x-axis is aligned with the direction of the sheet's motion, while the y-axis is taken normal to it, as illustrated in Figure a. The surface is considered permeable, with a wall mass transfer velocity defined as $v_w = -v_0$, where $v_0 > 0$ represents suction. The effects of viscous dissipation and Joule heating are assumed to be negligible.

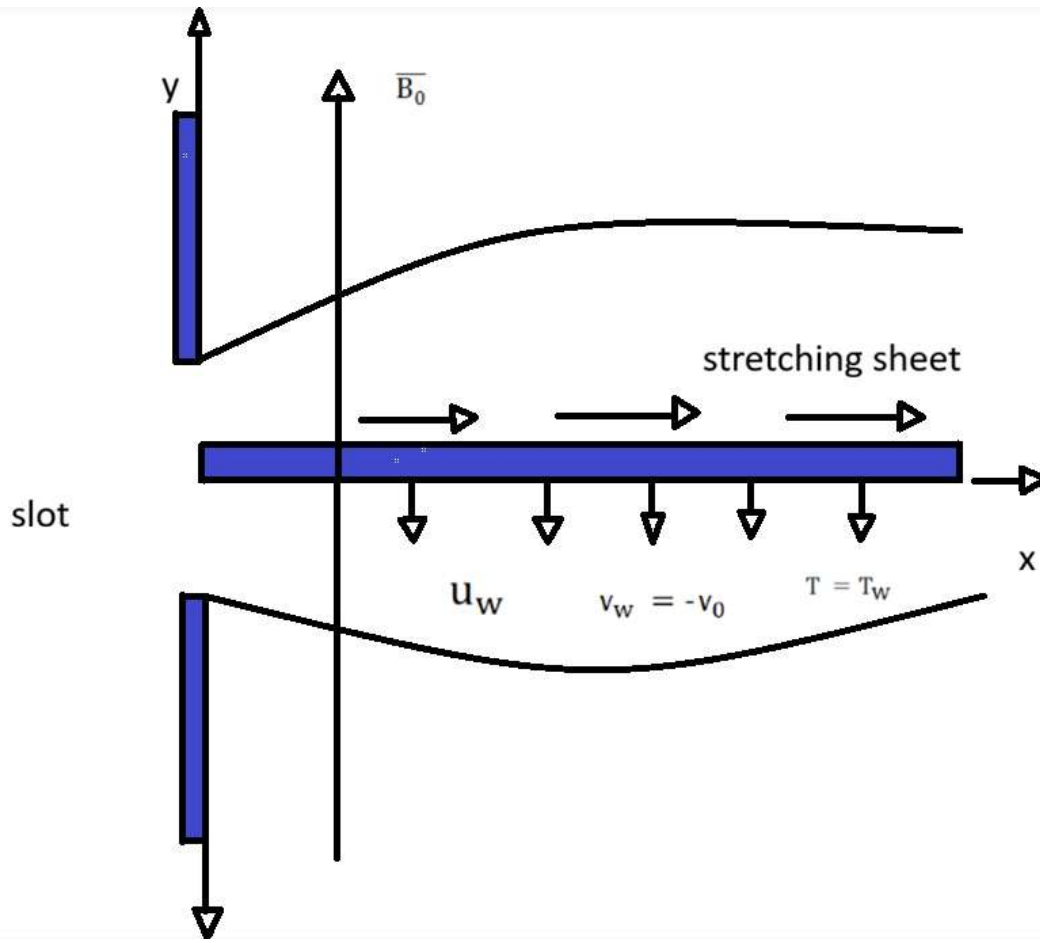


Fig:a Schematic diagram of the flow

$$u \frac{\partial u}{\partial x} + v \frac{\partial v}{\partial y} = 0, \dots \dots \dots (1)$$

$$u \frac{\partial u}{\partial x} + v \frac{\partial v}{\partial y} = \nu_{hnf} \frac{\partial^2 u}{\partial y^2} - \frac{\sigma_{hnf}}{\rho_{hnf}} B_0^2 u, \dots \dots \dots (2)$$

$$u \frac{\partial T}{\partial x} + v \frac{\partial T}{\partial y} = \frac{k_{hnf}}{(\rho C_p)_{hnf}} \frac{\partial^2 T}{\partial y^2}, \dots \dots \dots (3)$$

With boundary condition

$$u(x,0) = U_w(x) = cx,$$

$$v(x,0) = -V_0, T(x,0) = T_w$$

$$u(x,\infty) \rightarrow \infty, T(x,\infty) \rightarrow \infty,$$

The velocity components along the x- and y-directions are represented by u and v , respectively, where c is a constant. The parameters ν_{hnf} and ρ_{hnf} denote the kinematic viscosity and density of the hybrid nanofluid. Similarly, k_{hnf} , σ_{hnf} , and $C_{p\,hnf}$ correspond to the thermal conductivity, electrical conductivity, and specific heat at constant pressure of the

hybrid nanofluid, respectively. The term B_0 represents the strength of the applied uniform magnetic field, while v_0 indicates the suction velocity, with $v_0 > 0$. Furthermore, T denotes the fluid temperature, T_w is the temperature at the wall, and T_∞ refers to the ambient temperature far from the surface.

Table 1: Thermal characteristics of Cu, Al_2O_3 and H_2O are also mentioned (see Ref. [9])

Physical properties	Fluid phase (H_2O)	Copper (Cu)	Aluminium (Al_2O_3)
$P(\text{kg}/\text{m}^3)$	997.1	8933	3970
$c_p(\text{J}/\text{kgK})$	4179	385	765
$K(\text{W}/\text{mk})$	0.613	401	40
$\Sigma(\text{s}/\text{m})$	$5.5 \cdot 10^{-6}$	$5.96 \cdot 10^7$	$1 \cdot 10^{-10}$

Table 2: Thermophysical properties of Hybrid Nanofluid

Properties	Hnf	MNF
Density	$\rho_{Hnf} = (1 - \hat{\phi}_b)[(1 - \hat{\phi}_a)\rho_f + \hat{\phi}_a\rho_{sa}] + \hat{\phi}_b\rho_{sb} + \hat{\phi}_b\rho_{sb}$	$\rho_{nf} = (1 - \hat{\phi}_a)\rho_f + \hat{\phi}_a(\rho_{sa})$
Heat Capacity	$(\rho_{c_p})_{Hnf} = 1 - \hat{\phi}_b \{ [(1 - \hat{\phi}_a)(\rho_{c_p})_f + \hat{\phi}_a(\rho_{c_p})_{sa}] \} + \hat{\phi}_b(\rho_{c_p})_{sb}$	$(\rho_{c_p})_{nf} = [(1 - \hat{\phi}_a)(\rho_{c_p})_f + \hat{\phi}_a(\rho_{c_p})_{sa}]$
Viscosity	$\mu_{Hnf} = \frac{\mu_f}{(1 - \phi_a)^{2.5} * (1 - \phi_b)^{2.5}}$	$\mu_{nf} = \frac{\mu_f}{(1 - \phi_a)^{2.5}}$
Thermal conductivity	$\frac{K_{Hnf}}{K_{bf}} = \frac{k_{sb} + (n - 1)k_{bf} - (n - 1)\phi_b(k_{bf} - k_{sb})}{k_{sb} + (n - 1)k_{bf} + \phi_b(k_{bf} - k_{sb})}$	$\frac{K_{nf}}{K_f} = \frac{k_{sa} + (n - 1)k_f - (n - 1)\phi_a(k_f - k_s)}{k_{sa} + (n - 1)k_f + \phi_a(k_f - k_{sa})}$

Cu+Al2o3/water	Skin Friction	Skin Friction	Cu/Water	Skin friction	Skin Friction
	Nachtsheim–Swigert shooting iteration	Bvp4c Method		Nachtsheim–Swigert shooting iteration	Bvp4c Method
$\phi_2=0.005$	-3.335263	-3.335242	$\phi_2=0.005$	4.008188	4.008166
0.02	-3.503772	-3.503743	0.02	4.018891	4.018673
0.04	-3.735916	-3.735878	0.04	4.03268	4.03261
0.06	-3.97734	-3.977275	0.06	4.046563	4.046569
$M^2=0$	-1.973957	-1.973853	$M^2=0$	4.24128	4.242101
1	-2.554136	-2.554089	1	4.16862	4.168237
4	-3.735916	-3.735916	4	4.032618	4.03261
9	-5.084042	-5.084011	9	3.902395	3.902398
S=0	-3.310532	-3.310516	S=0	1.635836	1.635785
0.5	-3.735916	-3.735878	0.5	4.032618	4.03261

1	-4.208702	-4.208639	1	6.705384	6.705411
1.5	-4.726	-4.725909	1.5	9.49825	9.498298

Table 3. summarizes the variation of the skin friction coefficient and Nusselt number for Cu/water and Cu–Al₂O₃/water hybrid nanofluids.

Cu+Al ₂ O ₃ /water	Nusslet number	Skin Friction	Cu/Water	Nusslet number	Nusslet number
	Nachtsheim–Swigert shooting iteration	Bvp4c Method		Nachtsheim–Swigert shooting iteration	Bvp4c Method
$\phi_2=0.005$	4.008188	4.008166	$\phi_2=0.005$	3.966018	3.966011
0.02	4.018891	4.018673	0.02	3.97434	3.974341
0.04	4.03268	4.03261	0.04	3.98537	3.985388
0.06	4.046563	4.046569	0.06	3.996422	3.996457
$M^2=0$	4.242128	4.242101	$M^2=0$	4.132241	4.132257
1	4.168262	4.168237	1	4.081784	4.081793
4	4.032618	4.03261	4	3.985374	3.985388
9	3.902395	3.902398	9	3.888601	3.888609
S=0	1.635836	1.635785	S=0	1.531489	1.531491
0.5	4.032618	4.03261	0.5	3.985379	3.985388
1	6.705384	6.705411	1	6.750319	6.750371
1.5	9.49825	9.498298	1.5	9.638723	9.638745

Table 4. summarizes the variation of the Nusselt number for Cu/water and Cu–Al₂O₃/water hybrid nanofluids.

Pr	Present value of Nusslet number	Previous value
2	0.911358	0.91135
6.13	1.759687	1.75968
7	1.895407	1.8954
20	3.353952	3.3539

Table 5. Comparative analysis of the numerical values of the dimensionless temperature gradient at the wall, $-\theta'$ (0)

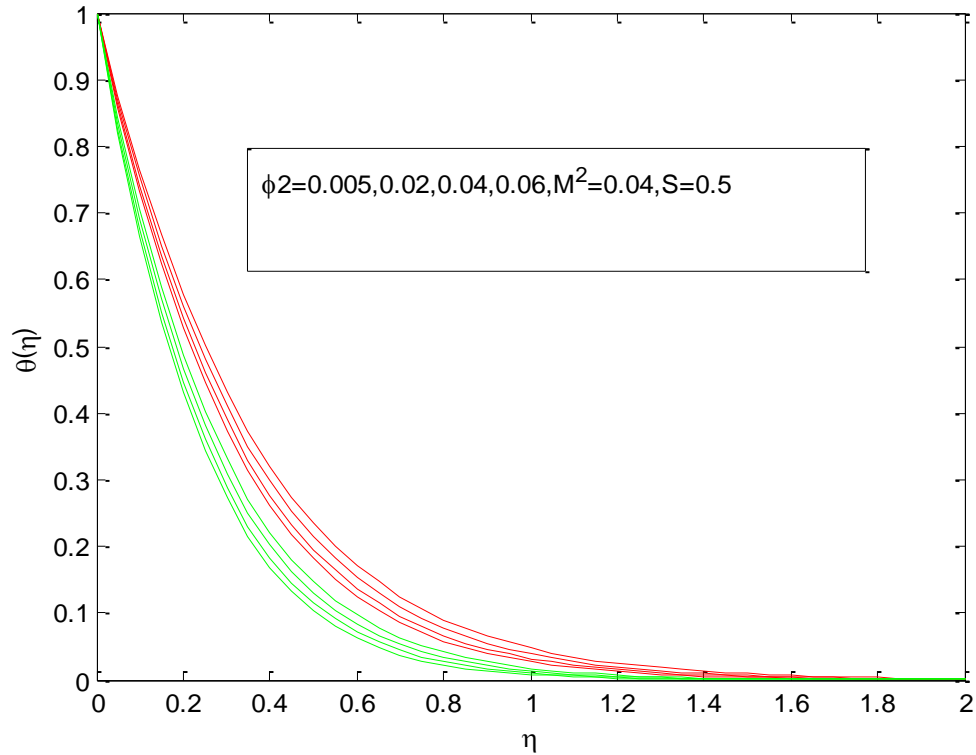


Fig:1 Temperature variation with different ϕ_2 parameters. (Green-Cu/Water, Red-Cu+Al₂O₃/Water)

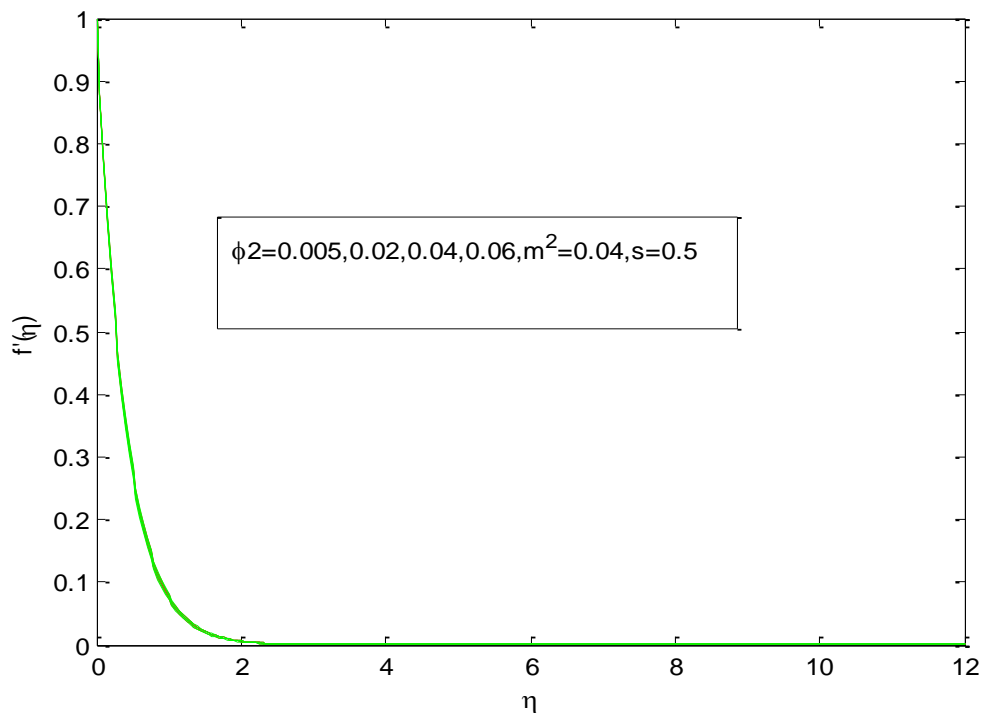


Fig.2 Velocity variation with different ϕ_2 parameters. (Green-Cu/Water, Red-Cu+Al₂O₃/Water)

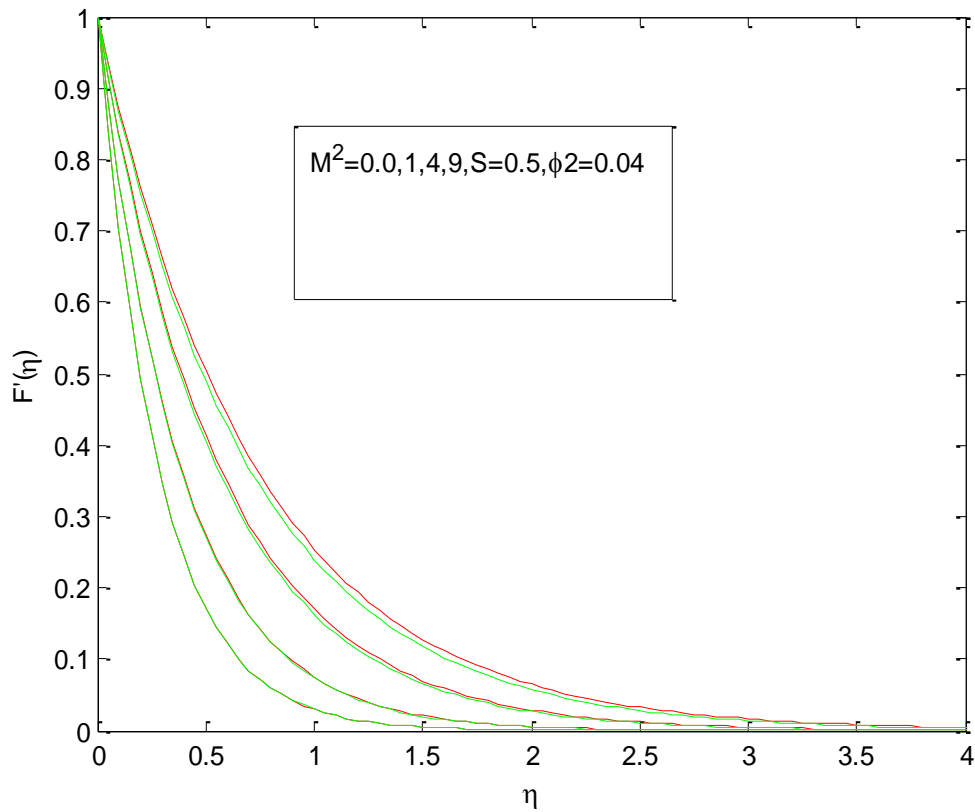


Fig.3 Velocity profiles for varying magnetic (Green-Cu/Water, Red-Cu+Al₂O₃/Water)

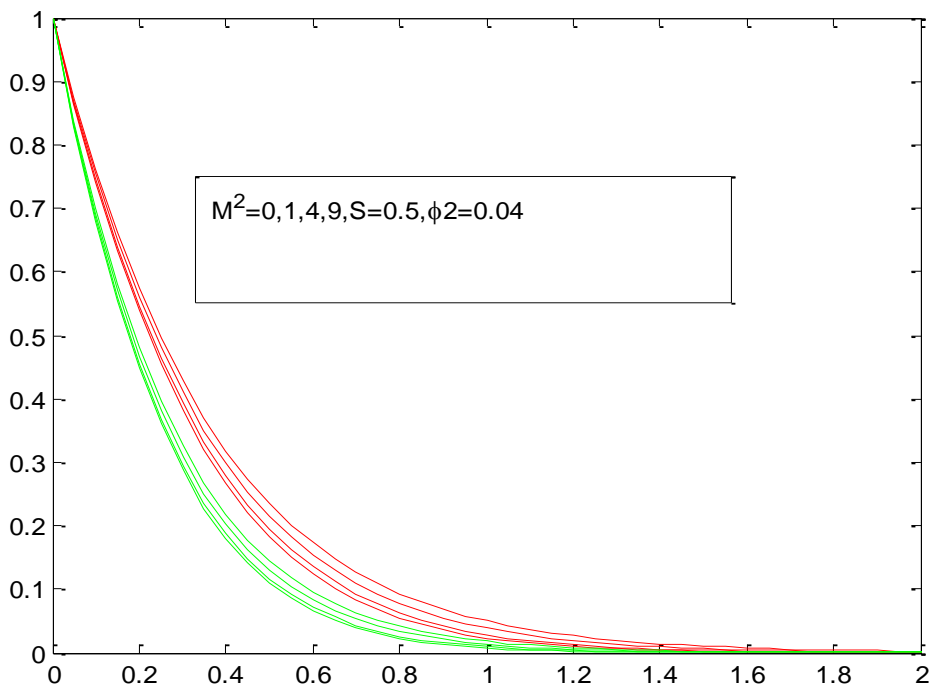


Fig.4 Temperature profiles corresponding to different values of Magnetic parameter (Green-Cu/Water, Red-Cu+Al₂O₃/Water)

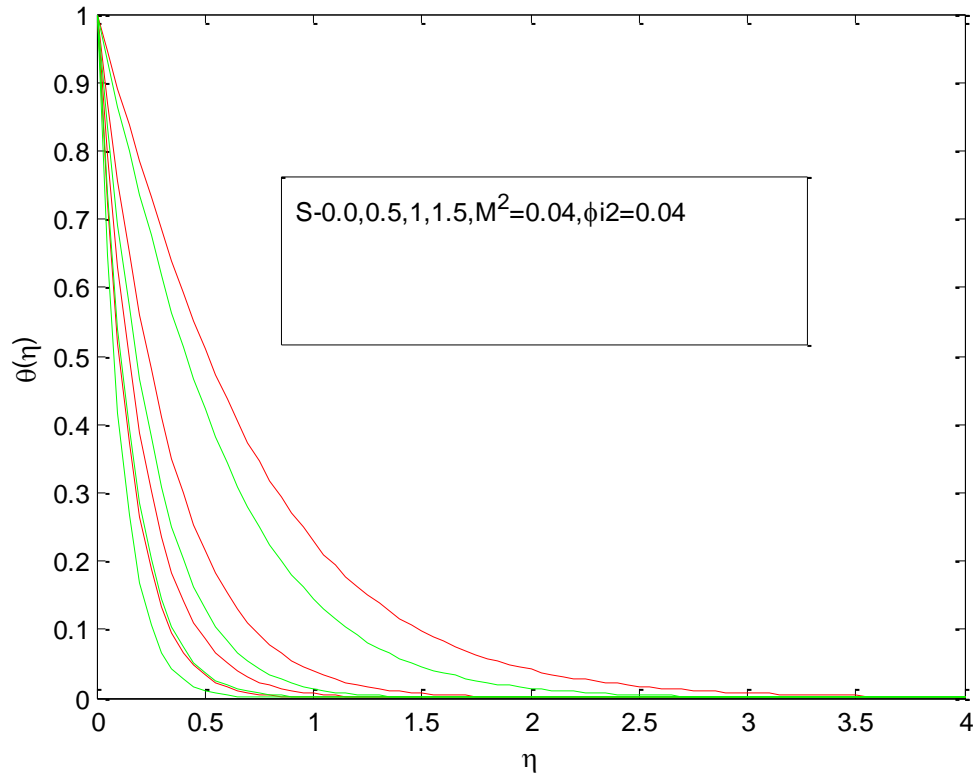


Fig.5Temperature profiles corresponding to different values of suction (Green-Cu/Water, Red-Cu+Al₂O₃/Water)

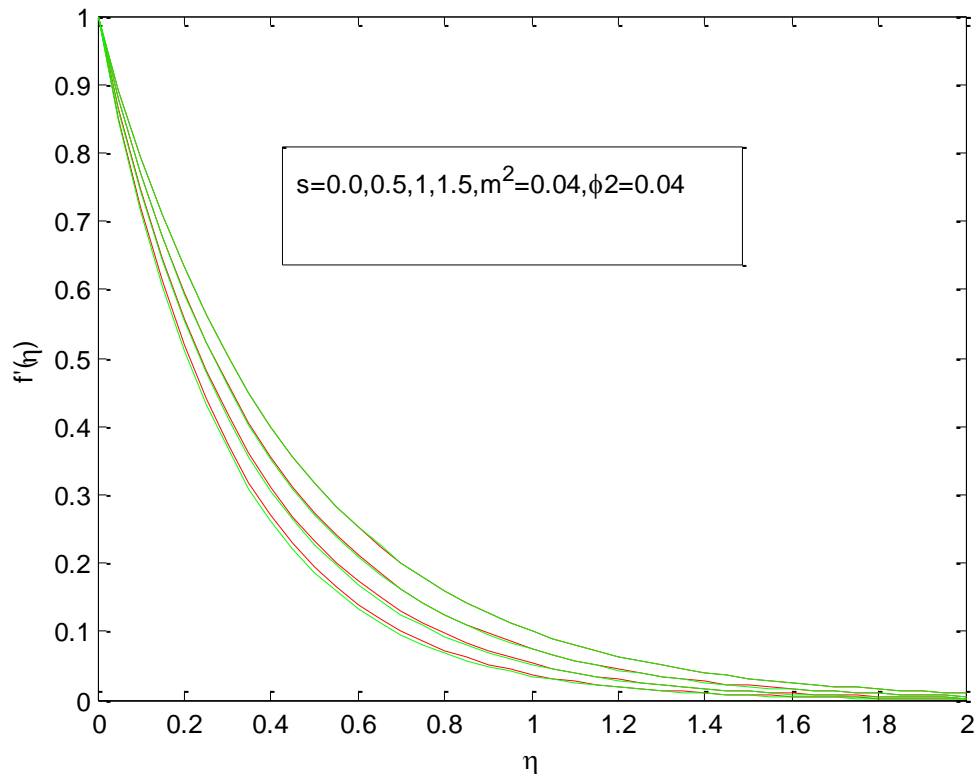


Fig.6 Velocity profiles corresponding to different values of Suction (Green-Cu/Water, Red-Cu+Al₂O₃/Water)

Result and Discussion:

In this model, Al₂O₃ nanoparticles (ϕ_1) are first dispersed into the base fluid at a fixed solid volume fraction of 0.1 ($\phi_1 = 0.1$), which is maintained throughout the study. Subsequently, Cu nanoparticles (ϕ_2) are introduced in varying volume fractions to produce the hybrid nanofluid, Cu–Al₂O₃/water. For clarity, the resulting effective thermophysical properties of both the nanofluid and the hybrid nanofluid are summarized in Table 1.

The basic thermophysical properties of the nanofluid are obtained from well-established literature. The corresponding properties of the base fluid and nanoparticles at 25 °C are summarized in Table 2.

From Table 3, it can be observed that the skin friction coefficient decreases as the magnetic field increases, owing to the reduction in fluid velocity. The skin friction coefficient decreases with an increase in solid volume fraction for both conventional nanofluid and hybrid nanofluid systems. The table 4 also indicates that the rate of heat transfer declines with an increase in the magnetic field strength. Furthermore, it is evident that the dimensionless heat transfer rate is higher for the Cu–Al₂O₃/water hybrid nanofluid compared to the Cu/water nanofluid. The results indicate that increasing the nanoparticle volume fraction leads to an improvement in heat transfer rate, which is more pronounced in Cu–Al₂O₃/water hybrid nanofluid than in Cu/water nanofluid. Optimal heat transfer can be attained by carefully selecting the composition and proportion of the nanocomposite.

The numerical code is validated by comparing the results of the present study with those reported by Khan and Pop [18], as presented in Table 5. This comparison is carried out under the conditions of zero solid volume fractions ($\phi_1 = 0, \phi_2 = 0$), zero magnetic interaction parameter ($M^2 = 0$), and no suction

($S = 0$), for various values of the Prandtl number. It is observed that the present results are in excellent agreement with those findings

Influence of the nanoparticle volume fraction (ϕ_2):

The temperature profiles corresponding to different values of ϕ_2 for Cu–Al₂O₃/water and Cu/water are presented in temperature profile (Fig.1). From a physical standpoint, nanoparticles release energy in the form of heat. As the concentration of nanoparticles increases, more energy is generated, leading to a rise in temperature and a consequent thickening of the thermal boundary layer. A notably interesting outcome is identified from the present investigation of hybrid nanofluids. As the solid volume fraction increases, the incorporation of Cu nanoparticles into Al₂O₃/water, as well as their addition into pure water, is illustrated in velocity profile and temperature profile. It is observed that with increasing solid volume fraction, the velocity profile (Fig.2) $f'(\eta)$ decreases for both Cu–Al₂O₃/water and Cu/water, along with a reduction in the momentum boundary layer thickness. This behavior is attributed to the presence of highly conductive nanoparticles, which enhance the effect of the Lorentz force, thereby diminishing the fluid velocity as the solid volume fraction rises.

Influence of the magnetic effect:

The effects of the magnetic interaction parameter (M_2) on the velocity profile (Fig.3) $f'(\eta)$ and the dimensionless temperature profile (Fig.4) $\theta(\eta)$ are respectively. The application of a transverse magnetic field generates a Lorentz force due to the interaction between the magnetic field and the electric field in a moving electrically conducting fluid. It is observed that for both the hybrid nanofluid and the conventional nanofluid, an increase in magnetic field strength enhances the resistive force, which in turn reduces the fluid velocity and decreases the momentum boundary-layer thickness. Since the magnetic field tends to reduce the fluid velocity, it consequently raises the temperature and thickens the thermal boundary layer, as illustrated in velocity profile.

Influence of the suction parameter:

The influence of the suction parameter on the dimensionless velocity and temperature profiles is illustrated in temperature profile (Fig.5) and velocity profile (Fig.6). An increase in the suction parameter draws the fluid into the surface, altering the boundary layer structure. As a result, the velocity decreases with higher suction values for both Cu–Al₂O₃/water and Cu/water nanofluids. Moreover, the suction through the permeable sheet leads to a reduction in temperature as the suction parameter increases, as shown in Figure 8. This behavior can be attributed to the diminished friction between the fluid and the sheet due to the withdrawal of fluid from the flow region.

Conclusion:

A steady, two-dimensional, nonlinear laminar boundary-layer flow of an electrically conducting, incompressible, and viscous hybrid nanofluid over a permeable stretching sheet in the presence of a magnetic field has been analysed. In this study, a novel hybrid nanofluid, namely Cu–Al₂O₃/water, is utilized for investigation. In the limiting case where the solid volume fractions (ϕ_1 and ϕ_2), magnetic interaction parameter (M^2), and suction parameter (S) are all set to zero, the obtained results show excellent agreement with those reported by Khan and Pop [6] for various values of the Prandtl number.

Numerous industrial processes such as metal extrusion, hot rolling, glass blowing, glass fiber production, wire drawing, and stretching of fins involve significant heat generation during operation, which can adversely affect product quality. This issue can be mitigated by employing an appropriate fluid flow mechanism to ensure uniform heat transfer. The findings of the present study indicate that the application of hybrid nanofluids in a magnetic field enhances flow stability and significantly improves heat transfer rates, thereby leading to better product quality at reduced cost.

References:

1. K. Niihara, New design concept of structural ceramics/ceramic nanocomposites, *Nippon Seramikkusu Kyokai Gakujutsu Ronbunshi* 99 (1991), 974–982.
2. S. Jana, A. Salehi-Khojin, and W. -H. Zhong, Enhancement of fluid thermal conductivity by the addition of single and hybrid nano-additives, *Thermochim. Acta* 462 (2007), 45–55.
3. S. Suresh, K. P. Venkitaraj, P. Selvakumar, and M. Chandrasekar, Synthesis of Al₂O₃-cu/water hybrid nano-fluids using two step method and its thermo physical properties, *Colloids and Surf. A* 388 (2011), 41–48.
4. G. G. Momin, Experimental investigation of mixed convection with water-Al₂O₃ & hybrid nanofluid in inclined tube for laminar flow, *Int. J. Sci. Technol. Res.* 2 (2013), 195–202.
5. S. Suresh, K. P. Venkitaraj, P. Selvakumar, and M. Chandrasekar, Effect of Al₂O₃-cu/water hybrid nanofluid in heat transfer, *Exp. Therm. and Fluid Sci.* 38 (2012),
6. M. Baghbanzadeh, A. Rashidi, D. Rashtchian, R. Lotfi, and A. Amrollahi, Synthesis of spherical silica/multiwall carbon nanotubes hybrid nanostructures and investigation of thermal conductivity of related nanofluids, *Thermochim. Acta* 54 (2012), 87–94.
7. E. M. Sparrow and R. D. Cess, The effect of a magnetic field of free convection heat transfer, *Int. J. Heat and Mass Transfer* 3(1961), 267–2741.
8. L. J. Crane, Flow past a stretching plate, *Z. Angew. Math. Phys. ZAMP.* 21 (1970), 645–647.
9. H. I. Andersson and B. S. Dandapat, Flow of a power-law fluid over a stretching sheet, *Stability Appl. Anal. Continuous Media* 1 (1991), 339–347.
10. A. Chakrabarti and A. S. Gupta, Hydromagnetic flow and heat transfer over a stretching sheet, *Q. J. Mech. and Appl. Math.* 37 (1979), 73–78.
11. K. Vajravelu, Hydromagnetic convection at a continuous moving surface, *Acta Mech.* 72 (1988), 342–345.
12. S. Das, R. N. Jana, and O. D. Makinde, Magnetohydrodynamic mixed convective slip flow over an inclined porous plate with viscous dissipation and joule heating, *Alexandria Eng. J.* 54 (2015), 251–261

Copyright & License:



© Authors retain the copyright of this article. This work is published under the Creative Commons Attribution 4.0 International License (CC BY 4.0), permitting unrestricted use, distribution, and reproduction in any medium, provided the original work is properly cited.